Colloid Polym Sci (2004) 282: 892–900
DOI 10.1007/s00396-004-1101-8

ORIGINAL CONTRIBUTION

Bernd Smarsly
Daibin Kuang
Markus Antonietti

Making nanometer thick silica glass scaffolds: an experimental approach to learn about size effects in glasses

Received: 13 February 2004
Accepted: 12 March 2004
Published online: 21 April 2004

B. Smarsly · D. Kuang · M. Antonietti (✉)
Department of Colloid Chemistry,
Max-Planck-Institute of Colloids
and Interfaces, Research Campus Golm,
D-14424 Potsdam, Germany
E-mail:
markus.antonietti@mpikg-golm.mpg.de

Abstract A convenient method for the synthesis of very well defined porous silica glasses using ionic liquids as templates is presented. Depending on template concentration, these systems form a homologous series of mesoporous systems with diverse shapes, with the pores having constant thickness of about 2.4 nm. These nanostructures allow the analysis of the two-dimensional behavior of glasses, either from a liquid to be embedded in the pore or of the silica glass forming the wall. For the walls, the third reduced dimension can be varied in a systematic fashion. This approach is exemplified by analyzing the static glass structure of 2D-silica by WAXS.

Keywords Nanometer thicknesses · Silica glasses · Scaffolds · Size effects · Glasses · Porous silica glasses · Ionic liquids · Templates

Introduction

Glasses, both organic and inorganic, are not only an important class of materials omnipresent in culture, but also in very modern technology. Glasses are somewhat special as they possess a liquid like structure and a dynamic softening point, the glass transition, which is scientifically still not completely understood. It was early on that E.W. Fischer found that quantitative static X-ray measurements indicate the approach of the glass transition even in the glassy state [1] and laid the base of a fluctuation cluster description. In the later Fischer-Donth picture [2], the glass mobility is essentially prescribed by the dynamic coupling of local fluctuations, the correlation length of which diverges at about $T-T_g = 80$ K. The size of these coupled domains at the calorimetric glass transition are still under debate (and depend on the chemistry of the system) but can be roughly estimated to be about 5 nm. There is strong experimental evidence that a second relevant length [3] of the order of 20–200 nm exists which describes dynamic heterogeneities well above the glass transition, and it was Fischer again who tried to stress the relevance of this cluster-like mode for many properties of glassy polymers. As the existence of such dynamic large-scale heterogeneities is not a part of classical theories of the glass transition, their importance is only just being slowly revealed.

A convenient class of experiments to learn about the role of these length scales in glass forming liquids is to confine the glass process in porous media of various dimensionality and connectivity. Here, the size of the reduced dimensions must be well defined and small enough to interfere with the dynamic coupling effects of glass transition. First experiments in this direction were again reported by Fischer et al. [4, 5]. These experiment were later refined by Kremer et al. [6, 7] who was able to separate surface and volume effects in these pores and also analyzed dynamic effects in dependence of the size (variation between 2.5 nm and 7.5 nm). In coated nanopores and smaller nanopores, the dynamics was found to be much faster. In these papers the authors also tried to make an estimate for the minimal number of molecules to form a liquid, i.e., when the typical

behavior of a liquid really sets in. Very recent work by Patkowski and Fischer [8] using dynamic light scattering at similar systems showed an acceleration of the dynamics of such a system by up to six orders of magnitude, but a connection to a dynamic correlation length was not shown. It is the opinion of the present authors that the understanding even of those simplified systems is still far from being established, as contradictory experimental findings have been described.

Progress of these current experiments is not restricted by physics, but by the availability of better defined porous media. Most of the previous experiments were performed on etched glasses, which exhibit a sponge-like, disordered cubic structure created by the in-situ demixing of two inorganic species. Even the more ordered and defined structures of regular mesoporous silica made by surfactant templating turned out to be non-ideal systems, as the required regular mesoporosity is always accompanied by a significant contribution of unwanted microporosity, as shown by quantitative X-ray scattering and gas sorption experiments [9, 10] or pressure dependent SANS measurements [11].

Just very recently, some chemical recipes were found where silicas with both high pore regularity and pore definition (no micropores) could be produced, including a class of lamellar silica made in the presence of ionic liquids [12, 13]. Beside pore sizes in the range of 1.3–2 nm (depending on the template), it is the two-dimensional character of the pores which makes glass experiments in such systems exciting, including a better ability to model and to separate structural effects of material and pore structure.

It is the purpose of the present paper to describe the synthesis and characterization of these porous silicas in more detail, including a more careful analysis of the structure of the glassy silica walls, which has to be seen as a gas-confined glassy structure, too.

Experimental

The SAXS measurements were performed using a CuK_α rotating anode device with three-pinhole collimation, equipped with a 2D image plate detector.

WAXS measurements were carried out on a Bruker D8 instrument in symmetric reflection. Nitrogen sorption isotherms were obtained from a Micromeritics Tristar 3000 instrument. Transmission Electron Microscopy (TEM) images were taken with a Zeiss EM 912 Ω at an acceleration voltage of 120 kV. Samples were ground in a ball mill and taken up in acetone. One droplet of the suspension was applied to a 400 mesh carbon-coated copper grid and left to dry in air.

The synthesis of the surfactant (C_{16}mimCl) is derived from the procedure described [12]. Typically, 1-hexadecylchloride (65.24 g, 0.25 mol) was mixed with 1-methylimidazole (20.54 g, 0.25 mol). The mixture was put into a 250-ml flask, refluxed at 90 °C for 24 h, and then cooled down to room temperature. The pure C_{16}mimCl product was obtained by recrystallization in the THF solvent. After recrystallization and washing several times with THF, the crystalline C_{16}mimCl white powder was collected by vacuum filtration, and dried in air at room temperature. The purity was verified by NMR.

Preparation of mesoporous silica In a typical synthesis with C_{16}mimCl as template, tetramethylorthosilicate (TMOS) was used as the sol-gel precursor. 0.36 g (1.05 mmol) of C_{16}mimCl was dissolved in 2 ml of EtOH, then mixed with 2.0 ml of TMOS under mild magnetic stirring. After homogenization of the mixture, 1.0 ml of aqueous solution of 0.01 mol/l HCl as an acid catalyst was added dropwise. The resulting mixture was stirred for 30 min. Complete gelation was accomplished by leaving the sample in an open flask at room temperature. A transparent colorless silica monolith was obtained with no visible cracks and very high mechanical stability. The transparency of the hybrid materials strongly suggests the homogeneity of C_{16}mimCl in the silica matrix and the absence of phase separation between the IL and silica. C_{16}mimCl was removed from the silica by calcination of the sample at 550 °C for 5 h with a temperature ramp of 100 °C/h from room temperature to 550 °C. The final product was ground into powders for further characterization.

Results

Preparation and characterization of mesoporous silicas

The templating properties of the ionic-liquid surfactant to generate mesoporous silica was already examined in previous work [12], but details of the templating behavior had not been studied. Here, we also try to avoid by a slight change of the preparation condition, the $L_ß$-phase of the previous experiments. As the details of the phase behavior is not the concern of the present paper, we will report on that in a forthcoming contribution. As we want to make systems with a different thickness of the siliceous walls, a series of samples was prepared by changing the surfactant/SiO_2 weight ratio w_{surf}/w_{SiO_2}, applying the nanocasting method [14]. In essence, in this procedure a siliceous precursor (in this case tetramethoxysilicate, TMOS) is condensed within the hydrophilic domains of a lyotropic mesostructure. The template is then removed by calcination to give the pores.

The amount of surfactant of TMOS in the starting solution was varied from a maximum value, beyond which no well-defined mesostructure could be observed by small-angle X-ray scattering (SAXS), down to values where the silica is the clear majority phase. Both the pore sizes and wall thickness can be expected to change with the system composition.

Figure 1 shows the SAXS data of representative samples, the reflections indicating the presence of a well-defined 2D hexagonal mesopore/silica arrangement.

It is noteworthy that the SAXS data obey the Porod-law at larger scattering vectors s ($s = 2\sin\theta/\lambda$), which is characteristic of an almost perfect two-phase system (that is a material composed of two regions of constant electron densities) with sharp interface boundaries between silica and the voids. The presence of a pronounced Porod-law behavior is rarely seen in ordered mesoporous silicas and proves the high quality of these mesoporous silicas in terms of the pore uniformity, absence of micropores, and interface flatness, which is not the usual case [9, 10, 11, 15]. The excellent quality of the SAXS data therefore allowed a thorough analysis in terms of the pore sizes and especially the wall thickness, which was carried out using the ''chord-length distribution'' (CLD) formalism [16]. The CLD(r) can be extracted from SAXS data and is defined as the normalized second derivative of the Fourier-Transform of the SAXS data, which can be interpreted as the probability of finding chords (= connectors between two phases) of the length r. Recently, we have demonstrated for mesoporous materials with pore sizes larger than 5 nm that the shape of the CLD itself provides an illustrative and also quantitative measure of the mesopore size and wall thickness [9, 11].

Figure 2 shows the CLDs for three representative samples, namely the ones prepared from the highest and lowest surfactant concentrations and a sample obtained from a medium surfactant concentration. First, it is seen that the pore-to-pore distance decreases with increasing surfactant concentration (shift of the first minimum at around 3.8 nm to the left). Second, for each curve two maxima are observed, which are attributable to the pore size (right maximum at ca. 2.5 nm) and wall thickness (left maximum at ca. 1–2 nm), taking into account results from nitrogen sorption. Interestingly, the wall thickness decreases with the addition of surfactant, starting from ca. 1.4 nm, and the final wall thickness is only around 1 nm for the highest surfactant concentration. In contrast, the mesopore size does not change significantly and is about 2.4 nm.

Aside from the SAXS analysis detailed nitrogen analysis was performed to characterize the porosity of the materials. Figure 3 shows the nitrogen sorption isotherms of various samples, clearly showing the presence of a mesoporous material. Applying the BJH formalism to the desorption branch, we obtain mesopore sizes of around 2.4 nm, which is in excellent agreement with the CLD analysis. A suitable method to derive the wall thickness from sorption data of well-organized mesoporous materials was introduced by Zhao [17]. Taking the d-spacing from the SAXS data, the wall thickness can be determined via $a = 2/3^{1/2}\, d$, with the wall thickness = a − pore size. The data are summarized in the Table below, revealing a similar trend as observed

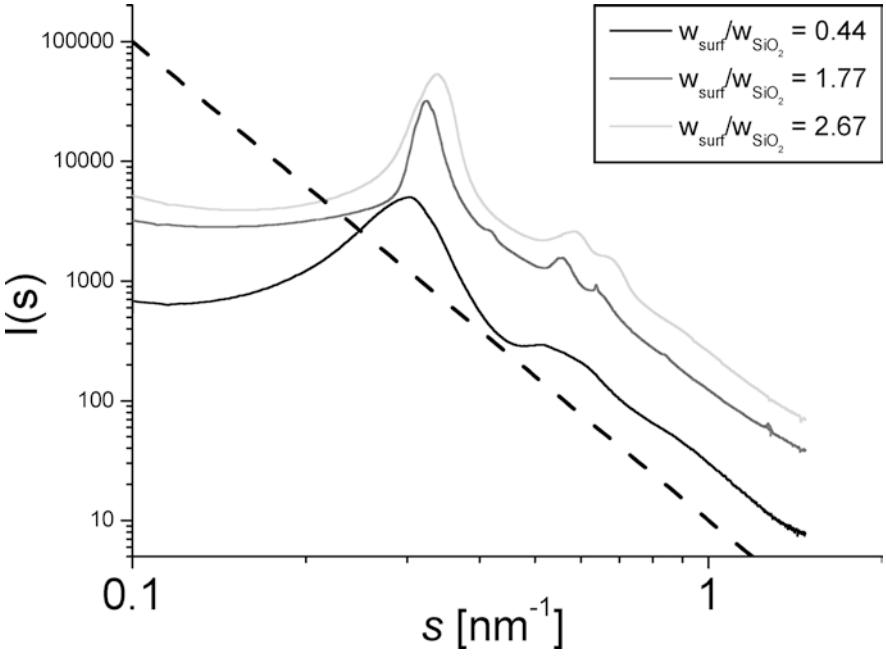

Fig. 1 SAXS curves of three mesoporous silicas, obtained using different surfactant concentrations. *Lower curve*: $w_{surf}/w_{SiO_2} = 0.44$, *middle curve*: $w_{surf}/w_{SiO_2} = 1.77$, *upper curve*: $w_{surf}/w_{SiO_2} = 2.67$. The *black dashed line* represents the Porod-law $I(s) = s^{-4}$

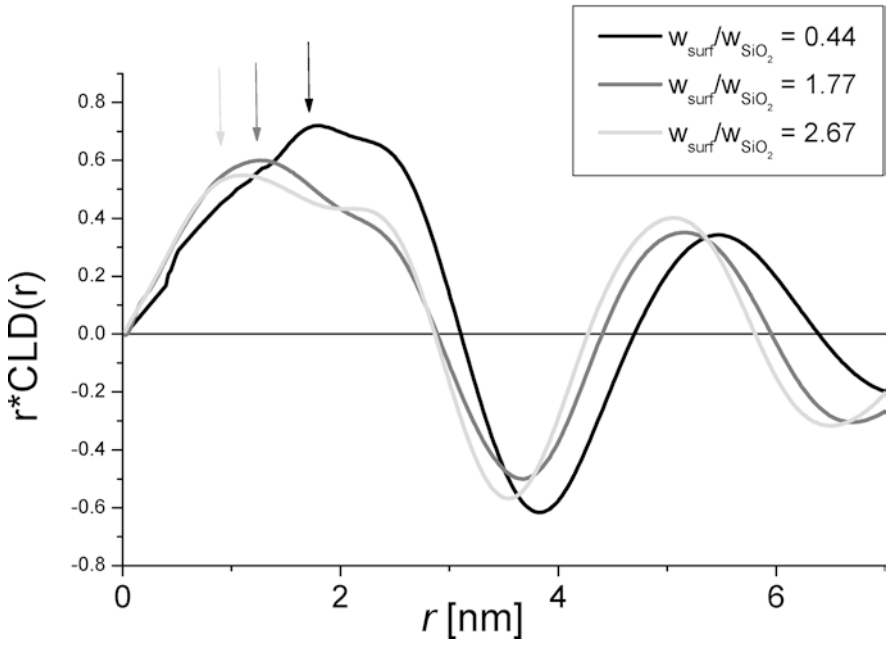

Fig. 2 Chord-length distributions (CLD) obtained from the SAXS curves in Fig. 1. The CLD is represented in the form r*CLD for better illustration. The *arrows* indicate the position of the maxima attributable to the wall thickness

from the SAXS evaluation: the wall thickness decreases with increasing surfactant concentration, the pore size remaining almost constant, but with slight decreasing. Surprisingly, for the present surfactant this trend is different from the results recently observed for block copolymer templated materials, where an increase in the surfactant concentration lead to an according increase in the mesopore sizes [18]. For block copolymer templating, changing the surfactant concentration was shown to result in a significantly different swelling of the hydrophilic PEO block and, thereby, to a different hydrophilic-hydrophobic balance. In the present case, the nature of the template, the ionic liquid, seems to make the self-assembly less sensitive towards changes in the hydrophilic-hydrophobic balance, as is seen in the almost constant mesopore size.

w_{surf}/w_{SiO_2}	Pore size (desorption) [nm]	BET surface area [m^2/g]	Pore volume [cm^3/g]	d value (SAXS) [nm]	Wall thickness [nm] (SAXS)
0.44	2.44	752	0.34	3.33	1.4 (1.4)
1.77	2.31	1552	0.71	3.08	1.2 (1.1)
2.67	2.38	1681	0.76	2.96	1.0 (1.0)

The extremely high regularity of the present materials can also be seen in TEM images. Figure 4 shows representative TEM images taken from the calcined materials reveal a highly regular channel system, with liquid crystalline order extending on the micron-scale. CLD formalism in combination with porosimetry therefore confirms the quite ideal structure of the present mesoporous silica. Thereby, these materials are ideal candidates to study the influence of the wall thickness on the internal wall structure.

Influence of the pore wall thickness on the internal wall structure

The silica walls of mesoporous materials consist of an amorphous network of silica tetrahedra, which, can be connected in various fashions, e.g., in the form of six-rings, eight-rings and other species. In this respect, there is no fundamental difference between a silica glass and a mesoporous silica. Here we address the question if the decrease in the wall thickness down to molecular dimensions leads to a measurable effect on the distribution of the silica tetrahedra and, thus, the internal glass structure and mobility. Wide-angle X-ray diffraction (WAXS) represents a suitable tool to monitor fine changes in the wall structure, because it directly probes the interatomic distances present in the material. WAXS is widely used for the study of glassy materials, showing broad maxima. Amorphous SiO_2 was already subject to detailed WAXS studies [19, 20], using high-energy photon WAXS to achieve as high scattering values as possible (up to $s = 60\ nm^{-1}$), allowing a precise determination of the SiO_2 structure factor [21]. In the present case, we only focus on the first maxima observed in WAXS, which is related to the average Si-Si distance in amorphous SiO_2, that is the average distance of

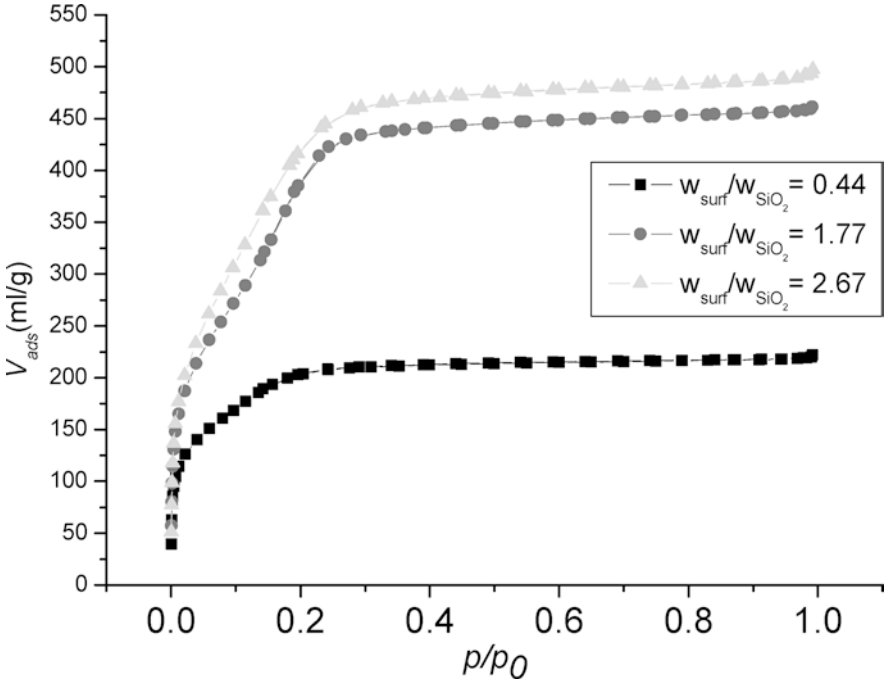

Fig. 3 Nitrogen sorption isotherms for mesoporous silicas, prepared using different weight ratios

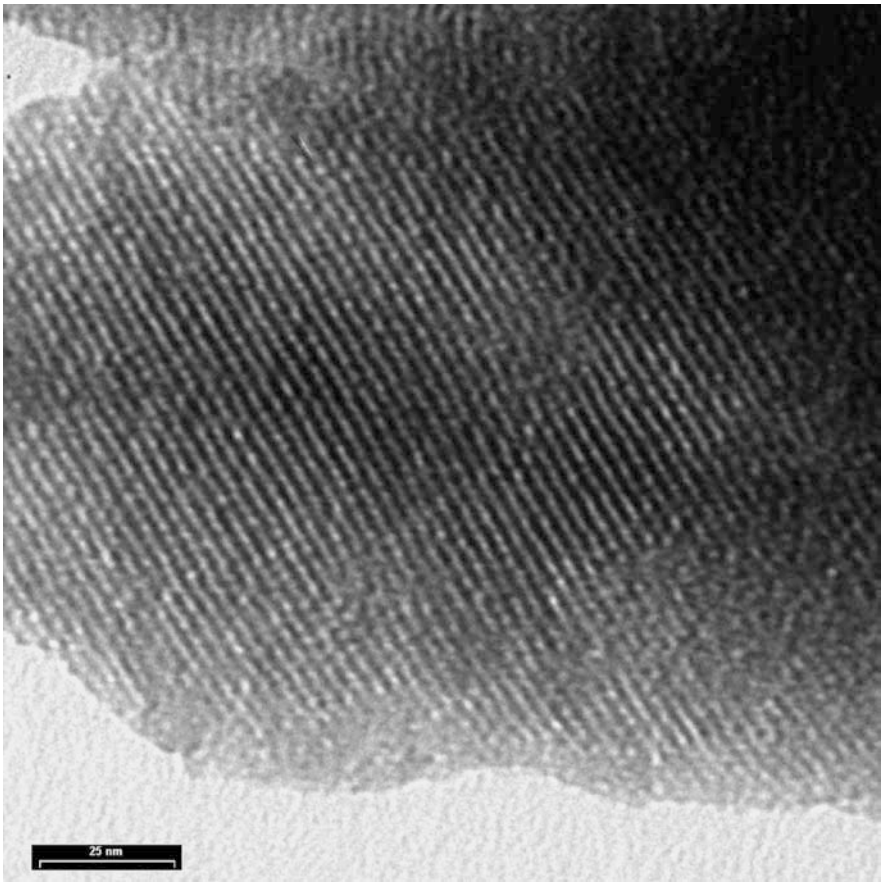

Fig. 4 TEM picture of one of the mesoporous silica (sample $w_{surf}/w_{SiO2} = 1.67$). The *scale bar* corresponds to 25 nm

two silica tetrahedra. Figure 5 shows the WAXS pattern for the present samples as a function of the surfactant/TMOS ratio. A small amount of a salt was added, serving as a standard for the position of the maxima. One silica sample was prepared without the addition of surfactant, thus corresponding to an almost non-porous silica glass for reference purposes. In all of the materials the characteristic first maximum was observed around $2\theta = 21.5$–$22°$, the value for the reference silica being in agreement with that observed for other SiO_2 glasses.

Interestingly, the position of the maximum shifts slightly, but systematically to higher 2θ values upon surfactant increase and, thus, upon decreasing the wall thickness. Since the samples were measured under comparable conditions, this shift itself already indicates a decrease in the average distance between two silica tetrahedra, i.e., a better packing in of the glass.

To come up with a more quantitative evaluation of the WAXS data, a "synthetic" approach was applied, fitting the data in the interesting region $2\theta = 10$–$70°$ by an empirical structure factor Z(s), providing a semi-quantitative measure for the average Si-Si distance. For Z(s) we have used the approach introduced by Wertheim et al., which turned out to be appropriate to simulate the SAXS of liquid-like structures, composed of isotropic objects [22, 23, 24]. As a main advantage, this approach is characterized by basic analytical algebraic expressions for Z(s). It must be stated that such WAXS data are usually measured up to very high s-values ($s = 40$ nm^{-1}), then are evaluated by determining the entire SiO_2 interference function s*(Z(s)−1), where Z(s) represents the lattice factor of the silica glass. The Fourier-transform of s*(Z(s)−1) results in the pair correlation function G(r), from which the radial distribution function P(r) is accessible. In the present case this procedure was not applicable, as the structure factor could not be measured up to very high s by our setup, thus leading to cut-off problems with the Fourier-Transform.

Prior to the analysis, the data were corrected for background scattering (*bg*), polarization ($P(s)$), and the absorption factor $A(s)$, taking into account the diffraction geometry (symmetric reflexion).

Hence, the final formula to analyze the WAXS data was $I(s) = A(s)\ P(s)\ f(s)\ Z(s) + bg$.

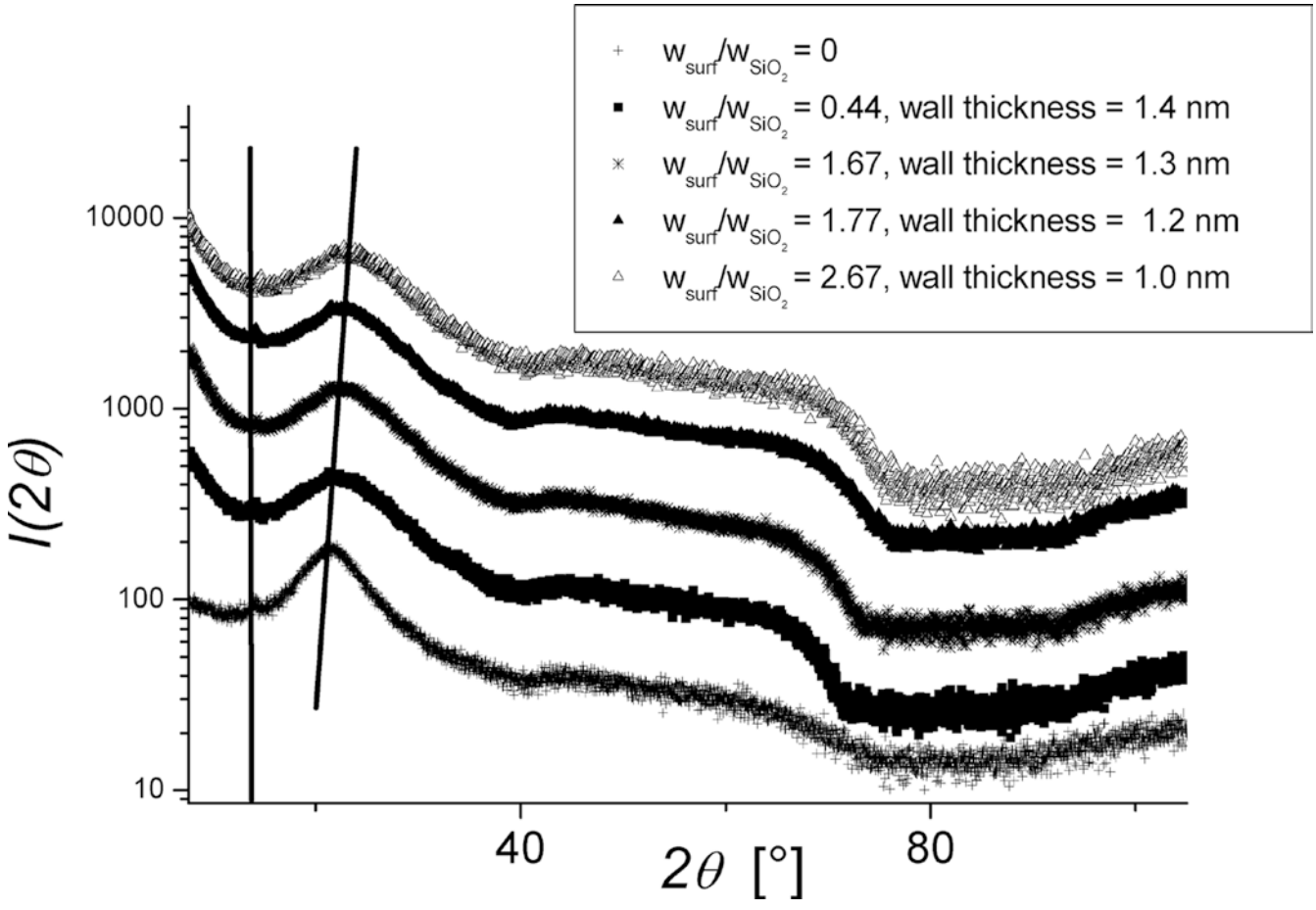

Fig. 5 WAXS diffractograms for various mesoporous silicas as a function of the pore wall thickness (surfactant concentration). The *black line* at $2\theta = 13°$ shows the position of a reference peak

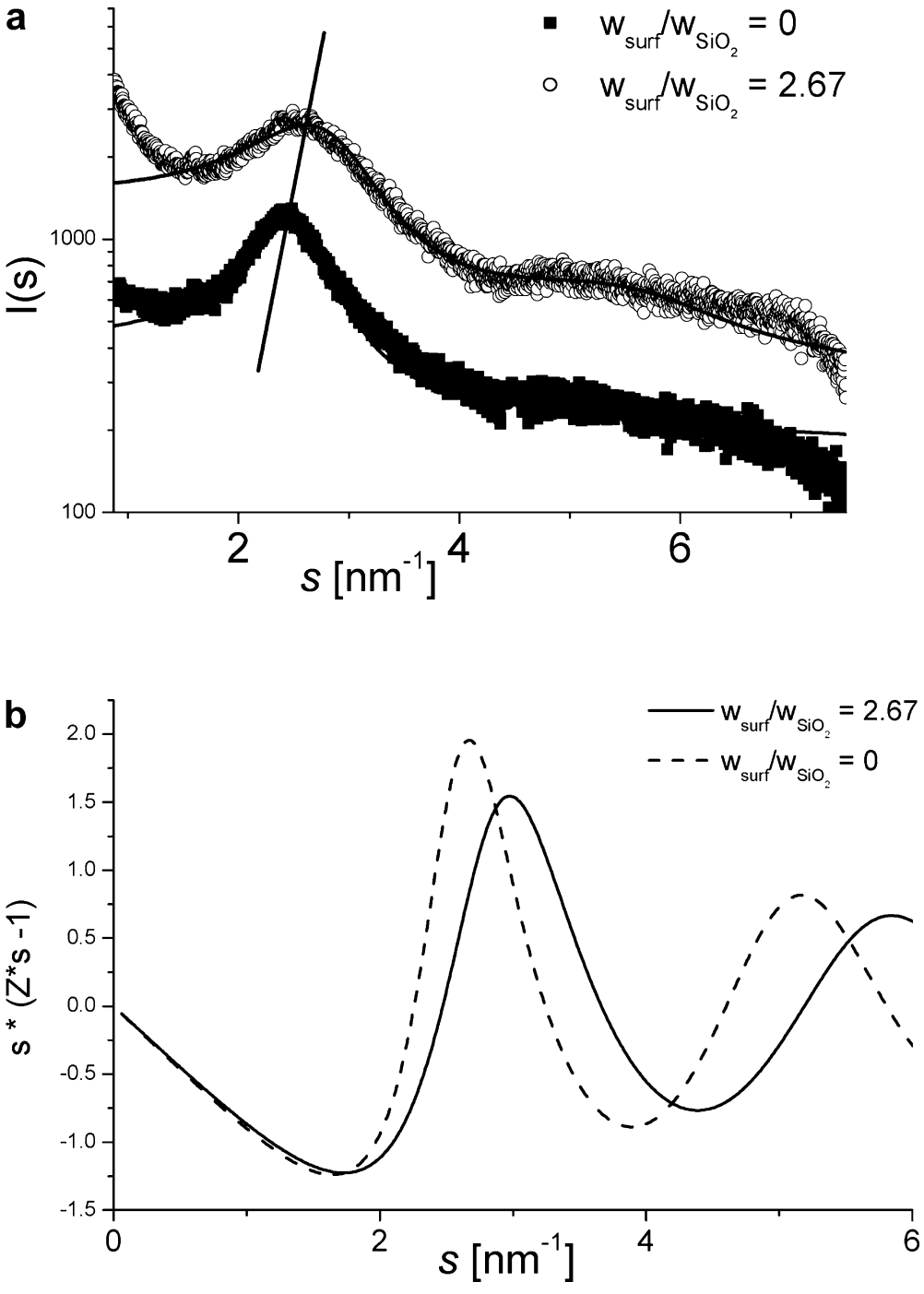

Fig. 6 a Fitting of the WAXS curves of the non-templated silica (*lower curve*) and the sample showing a lowest wall-thickness (1 nm) around the main peak at $2\theta = 22°$ using an approximation for the structure factor. **b** Interference functions obtained from the curves in a

The form factor *f(s)* of SiO_2 was exactly taken into account using data taken from the Tables of the International Union of Crystallography [25].

As seen in Fig. 6a, the data can be reasonably fitted by this approach, providing usable values for the average Si-Si distance. Figure 6b shows the coupled interference function s*(Z(s)−1), the maximum at ca. $s = 3$ nm^{-1} corresponding to the average Si-Si distance, which is in accordance with recently reported values. Comparing the samples with the lowest and highest surfactant concentration, a significant decrease well beyond experimental error of ca. 4% is observed in the maximum position, being attributable to the average distance between two silica tetrahedra. The difference of the densities of amorphous silica ($\rho \approx 2.2$ g/cm^3), crystobalite ($\rho \approx 2.65$ g/cm^3), and crystalline quartz

($\rho \approx 2.65$ g/cm^3) is sufficiently high to allow such a compression in the amorphous state.

It has to be emphasized that our procedure is not able to determine the absolute value of the Si-Si distance with sufficient precision, which would be achievable by a high-energy WAXS setup. However, it can be safely stated that a correlation exists between the thickness of the silica walls and the average distance between two silica tetrahedra. The thinner the silica walls get, the more the silica matrix tends towards a higher internal packing density. Higher densities would be coupled (according to the free volume model) to slower relaxations and a higher overall T_g. That way, a potential size effect on glass transition dynamics would be overlaid by a counterbalancing structural effect, explaining the widespread and partly inconsistent results found in the literature for confined glasses. A possible plausibilization of this effect is well known ageing of glasses which takes place on a logarithmic timescale and makes a quantitative comparison even between systems with similar composition without defining tempering protocols difficult. If this ageing is simply accelerated in the low-dimensional systems, one would compare the properties a non-relaxed three-dimensional glass with a relaxed two-dimensional glass, which is not feasible to do.

Conclusion and outlook

In the present study, mesoporous silicas were prepared by the nanocasting of a special ionic liquid. SAXS, nitrogen sorption, and TEM demonstrate that the materials under study represent an example for a unusually well ordered mesoporous silicas with an extremely high degree of perfection in terms of the packing, size, and morphology of the mesopore structure. A new method for the SAXS analysis, based on the CLD concept, allowed a precise determination of the pore wall thickness and pore size with 0.1 nm precision. Systematic variation of the volume fraction of template only resulted in a continuous variation of the silica wall thickness, whereas the pore size stayed constant. At the highest template concentration, a macroscopic sample was produced where however all the silica glass is part of thin pore walls of only about 1 nm. This thickness is only about 2.5–3 times the size of a silica tetrahedron, that means the whole sample is apt to show confinement effects on the structure (and dynamics) of glasses.

As seen directly in wide-angle X-ray scattering (WAXS) experiments, but also more clearly in the transformed interference functions, the small thickness seems to allow a higher density of the silica network. This is possibly explained by the way the silica tetrahedra are connected in the glassy structure, which obviously is less subject to topological confinements in lower dimensions. Usually, a wide variety of species such as 6- or 8-membered rings (and larger) can be observed, hosting areas of ''free volume'' and bigger voids which can be characterized by gas sorption as micropores. The latter are definitely absent in the present silica.

The details of this compaction of silica glasses plus a quantitative relation to the wall thickness has to be studied in further detail in forthcoming work by complementary techniques such as high-energy WAXS and Raman spectroscopy. In addition, we also intend to analyze the structure and architectural density of organic glasses confined in such porous media.

References

1. Wendorff JH, Fischer EW (1973) Kolloid-Z Z Polym 251:876–883
2. Fischer EW, Donth E, Steffen W (1992) Phys Rev Lett 68:2344–2346
3. Fischer EW (1993) Physica A 201:183–206
4. Schuller J, Melnichenko YB, Richert R, Fischer EW (1994) Phys Rev Lett 73:2224–2227
5. Schuller J, Richert R, Fischer EW (1995) Phys Rev B 52:15232–15238
6. Arndt M, Stannarius R, Groothues H, Hempel E, Kremer F (1997) Phys Rev Lett 79:2077–2080
7. Kremer F, Huwe A, Arndt M, Behrens P, Schwieger W (1999) J Phys Condens Matter 11:A175-A188
8. Patkowski A, Ruths T, Fischer EW (2003) Phys Rev E 67:Art No 021501
9. Göltner CG, Smarsly B, Berton B, Antonietti M (2001) Chem Mater 13:1617–1624
10. Smarsly B, Polarz S, Antonietti M (2001) J Phys Chem 105:10473–10483
11. Smarsly B, Göltner CG, Antonietti M, Ruland W, Hoinkis E (2001) J Phys Chem 105:831–840
12. Zhou Y, Antonietti M (2003) Adv Mater 15:1452–1455
13. Zhou Y, Antonietti M (2003) Chem Commun 2564–2565
14. Polarz S, Antonietti M (2002) Chem Commun 2593–2604
15. Smarsly B, Yu K, Brinker CJ (2003) Detailed investigation of the microporous character of mesoporous silicas as revealed by small-angle scattering techniques. In: Nanotechnology in mesostructured materials—studies in surface science and catalysis. Elsevier Science BV, Amsterdam, pp 295–298
16. Burger C, Ruland W (2001) Acta Crystallogr Sect A 57:482–491
17. Zhao D et al. (1998) Science 297:548–552
18. Thomas A, Schlaad H, Smarsly B, Antonietti M (2003) Langmuir 19:4455–4459
19. Mozzi RL, Warren BE (1969) J Appl Crystallogr 2:164–172

20. Konnert JH, Karle J, Ferguson GA (1972) Acta Crystallogr Sect A 28:128–129
21. Schlenz H, Neuefeind J, Rings S (2003) J Phys Condens Matter 15:4919–4926
22. Wertheim MS (1963) Phys Rev Lett 10:321–323
23. Wertheim MS (1965) J Chem Phys 43:1370–1380
24. Ashcroft NW, Lekner J (1966) Phys Rev 145:83–90
25. Wilson AJC, Prince E (eds) (1999) International tables for crystallography, 2nd edn. Kluwer Academic Publishers, Dordrecht